Maejo Int. J. Sci. Technol. **2021**, *15*(03), 273-292

Maejo International Journal of Science and Technology

ISSN 1905-7873

Available online at www.mijst.mju.ac.th

Review

A review on left ventricle segmentation and quantification by cardiac magnetic resonance images using convolutional neural networks

Zakarya Farea Shaaf, Muhammad Mahadi Abdul Jamil* and Radzi Ambar

Faculty of Electrical and Electronic Engineering, Universiti Tun Hussein Onn Malaysia, 86400, Parit Raja, Batu Pahat, Johor, Malaysia

* Corresponding author, e-mail: mahadi@uthm.edu.my

Received: 27 May 2021 / Accepted: 1 December 2021 / Published: 8 December 2021

Abstract: The quantification of the left ventricle (LV) by cardiac magnetic resonance images (MRI) is critical in the diagnosis of cardiovascular diseases to estimate vital criteria such as ejection fraction, left ventricle mass and volume, stroke volume, and muscle thickness, which are the most significant indicators of cardiac functions. Manual segmentation of LV is a tedious task that requires considerable effort by experts. Therefore, it is necessary to develop precise models of LV and myocardium segmentation. Currently, the architectures of deep convolutional neural networks (CNNs) have been widely utilised with significant potential for automatic cardiac medical image segmentation and quantification. However, these architectures typically have different purposes with huge numbers of parameters and samples of data, resulting in varying accuracy and generalisation. This article describes extensive comparative research based on the previous assessments of the LV segmentation and quantification from MRI utilising CNN models and hybrid models (level-set/deformable models with CNN). Furthermore, this paper provides answers to why short-axis MRI datasets are used broadly in LV segmentation, why LV is the most vital chamber to be diagnosed in the heart, and why CNN algorithms are described as the most suitable algorithms in medical imaging semantic segmentation with extensive datasets.

Keywords: convolutional neural networks, deep learning, magnetic resonance images, left ventricle segmentation and quantification

Maejo Int. J. Sci. Technol. **2021**, *15*(03), 273-292

INTRODUCTION

The World Health Organisation declares cardiovascular diseases (CVDs) as the deadliest disease that threatens human life [1]. The American Heart Association estimates that human life expectancy can be extended by ten years if cardiovascular diseases can be prevented by effective diagnosis at an early stage. Thus, early detection of CVDs is a crucial factor in determining the suitable treatment that can improve human life and decrease the mortality rate. Cardiac magnetic resonance (MR) imaging is a major non-invasive imaging instrument for early diagnosis and prediction of CVDs, namely myocardial infarction [2], coronary heart disease [3], ischemic heart disease [4], arrhythmia [5], hypertrophy [6], congestive heart failure [7] and others. Cardiac MR imaging utilises computerised technology which consists of a powerful magnetic field and radio wave to develop explicit images of the heart's structure. In cardiac MR imaging, the quantification of various cardiac parameters on the left ventricle (LV) and right ventricle (RV) during cardiac contractility is necessary to diagnose underlying CVDs. Thus, before the quantification process, the segmentation of LV and RV using MR images (MRI) is crucial. Since manual segmentation of MRI is an arduous and laborious work that can result in human errors, various studies have developed computerised systems comprising segmentation algorithms that can automatically and precisely segment LV and RV contours [4–11]. However, these proposed algorithms face similar issues such as the outer and inner cardiac structures and the variation in the shape and size of RV and LV among patients.

Although Chen et al. [12] provided information on several deep learning methods for cardiac segmentation, they are used for whole heart segmentation from different dataset modalities, not primarily for LV segmentation from MRI, nor for comparative analysis of the state-of-the-art methods for LV quantification. Thus, this paper focuses on the review of segmentation and quantification methods from cardiac MRI of LV based on convolutional neural networks (CNNs) with the following objectives:

1. To show the reasons why LV is the most significant cardiac chamber to determine CVDs;
2. To determine the most suitable imaging techniques for segmenting LV on cardiac MRI;
3. To explain the trends and advantages of LV segmentation and quantification using CNNs.

ANATOMY OF LEFT VENTRICLE (LV)

The human heart is divided into four chambers: the upper chambers consist of the right atrium, which receives deoxygenated blood from the entire body; the left atrium receives oxygenated blood from the lungs, while the lower chambers consist of the RV that pumps blood to the lungs and the LV. The LV is the most important and largest chamber because it pumps oxygenated blood to the entire body. Most CVDs are identified from LV, which can be diagnosed from the LV mass, LV volume, wall thickness and ejection fraction directly derived from LV at end-diastole (ED) and end-systole (ES) phases [8]. To extract these features, the LV contours must be precisely defined by identifying the endocardium (interior contour) surrounding the LV cavity (blood pool) and the epicardium (external contour) of the LV cavity. Furthermore, the LV myocardium is thicker than the RV myocardium; thus, it is easier to segment the LV [13]. Since the LV pumps high-pressure oxygenated blood throughout the body, its wall is three times thicker than the RV's. A healthy LV cavity has an elongated ellipsoid shape surrounded by the myocardium that has a thickness ranging from 6 to 16 mm. A problematic LV, on the other hand, can be identified by

Maejo Int. J. Sci. Technol. **2021**, *15*(03), 273-292

the changes in its regional and global functions and shape. The LV's regional and global functions can be quantified by measuring the following indicators [11]:

i. LV end-diastolic volume: the mass of blood in LV, surrounded by myocardium, in the relaxation phase of the cardiac cycle;
ii. LV end-systolic volume: the mass of blood in LV, surrounded by myocardium, in the contraction phase of the cardiac cycle;
iii. LV stroke volume: the amount of ejected blood from the heart to the body at each contraction phase (the difference between i and ii);
iv. LV mass: the LV cavity during the ED and ES phases, surrounded by myocardium tissue;
v. LV ejection fraction: the percentage amount of blood pumped out of the heart at each beat;
vi. LV cardiac output: the amount of systemic blood flow per minute;
vii. LV wall thickness: the thickness of myocardium measured from short-axis images at the end-diastolic phase (Figure 1).

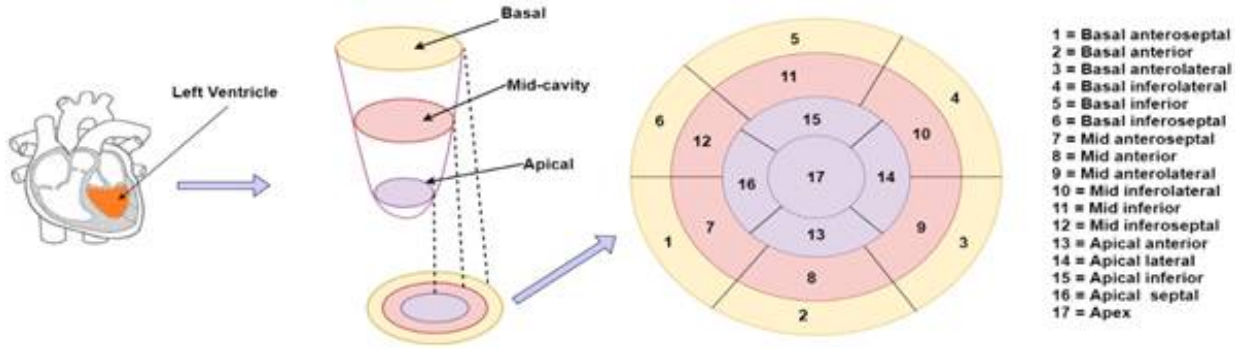

Figure 1. LV model with 17 segments of wall thickness

Currently, cardiac MRI are extremely useful in diagnosing CVDs due to their extensive ability to distinguish different types of tissues [9, 14]. Since short-axis MRI are easier to use than long-axis MRI, the former are utilised in many LV contour imaging techniques [13]. As a result, LV segmentation algorithms based on short-axis MRI have been long-established [15-17], particularly in deep learning algorithms [18-21]. A short-axis MR image is created by imaging perpendicular to the long axis with 8-10 slices throughout the cardiac cycle, and it comprises a stack of 2D MRI with a plane resolution of 5-10 mm.

CARDIAC MRI SEGMENTATION

As most CVDs are associated with irregular anatomical and structural indices of the heart, various cardiac diagnostic imaging techniques have been introduced, such as MR imaging, echocardiography, electrocardiography, computed tomography, ultrasound, positron emission tomography and single-photon emission computed tomography. Among these techniques, cardiac MR imaging is best suited for LV quantification because it gives reproducible measurements. Furthermore, when compared to other techniques such as single-photon emission computed tomography and computed tomography, cardiac MR imaging has the advantage of being radiation-free and capable of producing high-resolution images.

The literature clearly shows that MR imaging is the best technique for estimating LV parameters for instance LV volume, LV mass, ejection fraction and wall thickness. Cardiac MR

Maejo Int. J. Sci. Technol. **2021**, *15*(03), 273-292

imaging protocols include cine MR, tagged MR, flow MR, late gadolinium enhancement and perfusion MR, all of which provide different information [22]. The cardiac MR imaging planes are based on two axes: the short-axis view and the long-axis view. The standard imaging technique to segment LV is via a short-axis plane in which the imaging plane is perpendicular to the long-axis plane, and the long-axis crosses LV from base to apex, as shown in Figure 2. Since the heart is an active organ, images from cine MR imaging are acquired through the cardiac cycle and organised in dynamic sequences.

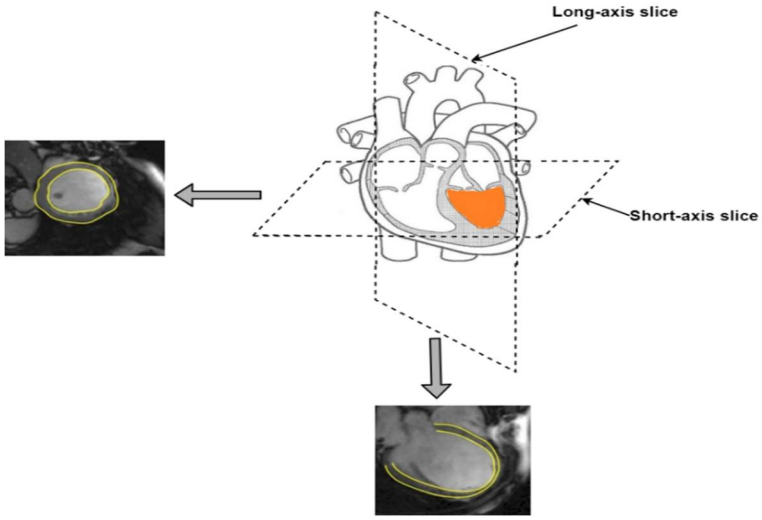

Figure 2. MR long-axis and short-axis views for LV segmentation

Among various protocols of cardiac MR imaging, cine MR provides good spatiotemporal resolution with high contrast between different tissues. Commonly, one sample has 20-30 consecutive frames, corresponding to 20- to 30-time points in the cardiac cycle. Typically, each frame contains 10-15 slices from base to apex [11]. Tagged MRI is used traditionally with a grid of tag lines imposed on the myocardium for LV motion estimation. However, the fading tags during the cardiac cycle make it difficult to identify in the last phase of sequences [23]. Flow MR is a protocol to cipher the information of velocity by adjusting the path of the gradient from +180º to -180º [22]. This protocol is applicable in measuring cardiovascular strain rate and flow. Perfusion MR is a technique by which the injection of a contrast agent (typically gadolinium) is applied to produce contrast-enhanced images [22]. The contrast agent flows with blood along the vessels to reach the target tissue. Late gadolinium enhancement MR is a vital method that estimates scar tissue in the myocardium [11]. The images acquired from this technique are from 6-mm short-axis slice thickness with a 4-mm gap for contrast enhancement. Then 0.10-0.15 mmol/kg of gadolinium was injected after a delay of 10-20 min. and subsequently, the images were collected.

The main step in analysing the motion and deformation of the heart is the segmentation of MRI sequences into frames that consist of different slices. The purpose of LV segmentation is to define the endocardial and epicardial contours. As depicted in Figure 3, the endocardial contour surrounds the LV cavity, the epicardial contour is between the myocardium and outer tissues (lungs, fat), and the myocardium is between these two contours.

Maejo Int. J. Sci. Technol. **2021**, *15*(03), 273-292

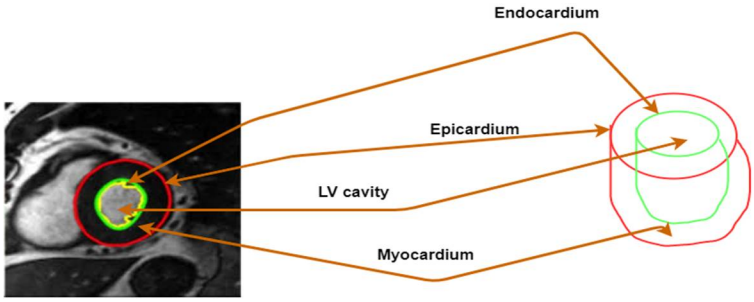

Figure 3. MR image of LV (left) and model of LV (right)

CONVOLUTIONAL NEURAL NETWORKS (CNNs)

CNNs are one of the most broadly used deep learning algorithms for image analysis. It is utilised for many different processes including classification [24], segmentation [25] and object detection [26]. As shown in Figure 4, a typical CNN has input and output layers, as well as a stack of layers that function between the input and output layers. These functional layers consist of three main layers, namely convolutional layer, pooling layer and fully connected layer. Typically, the convolutional layer includes kernels/filters followed by batch normalisation and a non-linear activation function (e.g. rectifier linear unit) that extracts feature maps from the input. Then the feature maps are followed by pooling layers for down sampling by disposing of unnecessary metrics to improve the generalisation and statistical efficiency of the model. Fully convolutional layers are involved in the dimension reduction of the previous layer's features and in finding the most related features for inference [12, 27].

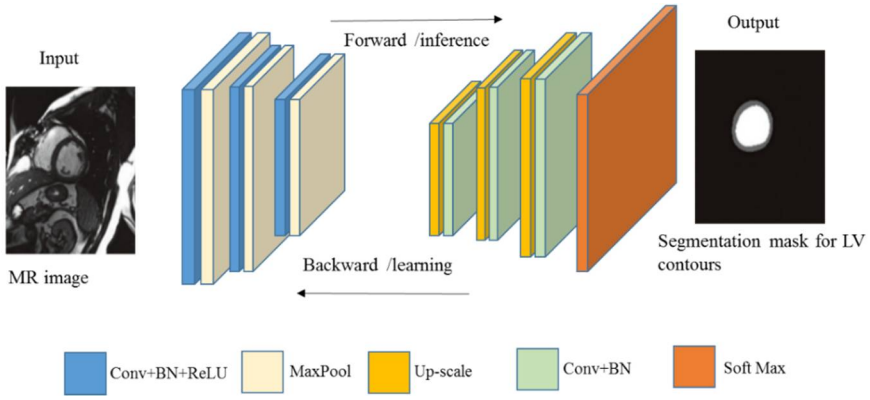

Figure 4. Layers of construction for complete CNN architecture (Conv= convolution, BN= batch normalisation, ReLU= rectified linear unit function and MaxPool= max pooling layer)

The network output is a fixed-size vector with elements for classification, object detection and segmentation purposes. There is well-documented literature on CNN algorithms assisting medical experts and physicians to diagnose breast cancer [28, 29] and brain tumours [30] as well as detect kidney disease [31], diabetic retinopathy [32], prostate cancer [33, 34] and cardiovascular diseases [35-38]. CNN models with different architectures are used for image segmentation and classification, including SegNet [39], AlexNet [32], ImageNet [24], GoogleNet and VGG. Full CNNs that track and label each pixel, such as the U-net model, are the most influential semantic segmentation CNN-based architecture in this field.

Maejo Int. J. Sci. Technol. **2021**, *15*(03), 273-292

Network Training

Neural network training is crucial before it is used to perform a specific function in image analysis. Therefore, standard training elements are required, for instance, data (images), optimiser algorithms and loss function to update the network's parameters via backpropagation algorithm. The main objective of the training process is to provide a suitable value for the parameters in the network by minimising the loss function using optimisation algorithms such as stochastic gradient descent [40] and adaptive moment estimation [41].

Common Loss Functions

The mean square error loss function (L_{MSE}) is the simplest for regression tasks, namely landmark detection, heart localisation and image reconstruction [12]:

$$L_{MSE} = \frac{1}{n}\sum_{i=1}^{n}\left(y_i - x_i\right)^2 \quad , \tag{1}$$

where y_i is the target vector value, x_i is the predicted vector value and n is the number of samples at each iteration.

For classification and segmentation tasks of images, the cross-entropy loss function (L_{CE}) is mostly used [12]:

$$L_{CE} = -\frac{1}{n}\sum_{i=1}^{n}\sum_{c=1}^{C} y_i^{\,c} \log\left(p_i^{\,c}\right) \quad , \tag{2}$$

where p_i predicts the probabilistic output, y_i is the target segmentation map, c is the number of each class and C is the number of all classes. For segmentation, the cross-entropy loss function represents errors of pixel-wise probability between predicted segmentation map and target map. Therefore, the soft-dice loss function (L_{Dice}) is applied to minimise the errors [42]:

$$L_{Dice} = 1 - \frac{2\sum_{i=1}^{n}\sum_{c=1}^{C} y_i^{\,c} p_i^{\,c}}{\sum_{i=1}^{n}\sum_{c=1}^{C}\left(y_i^{\,c} + p_i^{\,c}\right)} \quad . \tag{3}$$

Overfitting Reduction

Due to the difficulty of the training stages, the best approach to refining the precision of a deep neural network is to increase the number of layers and units by the level that increases the network's depth and width respectively [8]. As a result, high-quality model training can be performed with huge numbers of parameters, potentially causing overfitting. Deep learning accuracy can also be improved by presenting residual learning frameworks [43] for training by layer reformulation to learn residual functions related to the input layers rather than functions unrelated to the input layers. To deal with this problem one of the following step can be applied:

i. Weight regularisation: a technique in which weight penalties are added to the loss function;
ii. Dropout: a method that randomly drops neurons in each layer to enhance accuracy during training;
iii. Ensemble learning: a part of machine learning techniques where combined trained models are applied to produce better performance than that from a single model;
iv. Data augmentation: a manipulation of training samples to expand the types of training data (e.g. scaling, rotation and cropping);

Maejo Int. J. Sci. Technol. **2021**, *15*(03), 273-292

v. Transfer learning: reusing weights of a pre-trained model to initiate the new model's weights for a specific task.

Evaluation Metrics

A set of standardised metrics can be used to verify the performance of a proposed deep learning algorithm through a reproducibility approach. They are based on geometrical metrics, clinical performance and classification performance metrics as described below.

Geometrical metrics. The most important task in the LV segmentation method is to validate the precision of used algorithms. Many techniques utilise metrics (similarity functions) that compare the contours obtained from the segmentation algorithm with those derived from the ground truth segmentation [13].

Dice metric (DM) is a statistic technique for measuring the overlap between two regions, manually and automatically segmented contours, and is the mean Dice metric tool for detecting LV accuracy evaluation:

$$DM\left(S,M\right)=2\frac{\left|S\cap M\right|}{\left|S\right|+\left|M\right|}\ , \tag{3}$$

where *S* represents detected regions and *M* represents manual labels.

Jaccard index (J) has a similar function to DM. However, it maintains triangle inequality:

$$J\left(S,M\right)=\frac{\left|S\cap M\right|}{\left|S\cup M\right|}=\frac{DM\left(S,M\right)}{2-DM\left(S,M\right)}\ . \tag{4}$$

Hausdorff distance (d_H) is a method for formalising the space difference between regions:

$$d_H\left(S,M\right)=\max\left(\max_{p\in\partial S}d\left(p,\partial M\right),\max_{q\in\partial M}d\left(q,\partial S\right)\right)\ , \tag{5}$$

where $\left(p,\partial\right)$ represents the minimal interval between points p and q and contour ∂.

Clinical performance. To determine clinical performance indices, correlation, bias and standard deviation values are applied. These metrics are calculated using i) ED and ES volumes for LV and RV, expressed in mL/m^2; ii) ejection fractions, expressed in percentage of LV and RV; and iii) myocardium mass, expressed in g/m^2 , as listed by Bernard et al. [9].

Furthermore, as summarised by Hu et al. [44], critical parameters in LV functional measurements include LV mass in ES phase (LVM-SP), LV mass in ED phase (LVM-DP), LV ejection fraction (LVEF), LV end-diastolic volume in ED phase (LVEDV), LV end-systolic volume in ES phase (LVESV), LV stroke volume (LVSV) and cardiac output (CO):

$$LVEDV=V_{endo}^{ED}\ , \tag{6}$$

$$LVESV=V_{endo}^{ES}\ , \tag{7}$$

$$LVSV=V_{endo}^{ED}-V_{endo}^{ES}\ , \tag{8}$$

$$LVEF=\frac{\left(V_{endo}^{ED}-V_{endo}^{ES}\right)}{V_{endo}^{ED}}\times100\%\ , \tag{9}$$

$$LVMDP=(V_{epi}^{ED}-V_{endo}^{ED})\times p\ , \tag{10}$$

Maejo Int. J. Sci. Technol. **2021**, *15*(03), 273-292

$$LVMSP = (V_{epi}^{ES} - V_{endo}^{ES}) \times p \quad , \tag{11}$$

$$CO = (V_{endo}^{ED} - V_{endo}^{ES}) \times H_r \quad , \tag{12}$$

where V_{endo}^{ED} and V_{epi}^{ED} are endocardial and epicardial volumes at the ED phase respectively, V_{epi}^{ES} is the corresponding volume in the ES phase, H_r is the heart rate, and $p = 1.05\ g/cm^3$, the myocardial tissue density.

Classification performance. Classification evaluation metrics such as sensitivity (*sens*), specificity (*spec*), accuracy (acc) and precision (*prec*) are utilised to evaluate the performance of classification based on the confusion matrices [45]:

$$sens = \frac{TP}{TP + FN} \quad , \tag{13}$$

$$spec = \frac{TN}{TN + FP} \quad , \tag{14}$$

$$acc = \frac{TN + TP}{TN + TP + FN + FP} \quad , \tag{15}$$

$$prec = \frac{TP}{TP + FP} \quad , \tag{16}$$

where TP , TN , FP and FN are true positive, true negative, false positive and false negative respectively.

LV QUANTIFICATION AND SEGMENTATION VIA CNNs

Current automatic heart segmentation approaches can be classified as: pixel classification (clustering and Gaussian mixture model fitting) [46]; image-based methods (threshold and dynamic programming) [47]; deformable models (active contour and level set) [48]; statistical models (shape and appearance modelling) [49]; graph-based models (graph cut) [50]; and atlas models [51, 52] as organised in Figure 5.

These approaches are known as non-learning-based algorithms that promise results on a small dataset and achieve less performance with new data that are not in data training. Some of these methods are highly dependent on expert features that have limited ability to present various shapes and forms of specific anatomical organs such as the heart. As a result, to address these issues, learning-based methods such as deep learning have been investigated to achieve optimal results in this field [53]. Deep-learning-based algorithms are also broadly used to discover complex features automatically from data during segmentation and object detection. These features are learned in an end-to-end manner, making deep-learning-based algorithms effective in image analysis applications [12].

CNNs [54-56], fully convolutional network (FCN) [57], recurrent neural networks [5], auto-encoder [58] and generative adversarial networks [59] have demonstrated significant tasks in medical image analysis. FCN is a distinctive type of CNNs first proposed by Long et al. [60]. U-net [61] is the most suitable FCN architecture. Recurrent neural network is used for sequential data and has two popular models: long-short-term memory and gated recurrent unit [62]. Auto-encoder is a neural network that automatically learns compact latent representations of data [12]. The concept of generative adversarial network was introduced by Goodfellow [63], which consists of two

Maejo Int. J. Sci. Technol. **2021**, *15*(03), 273-292

networks: a generator network and a discriminator network. Creswell et al. [59] conducted extensive reviews of this model, which showed a prominent performance for segmenting tumours [64] and estimating the heart volume [65].

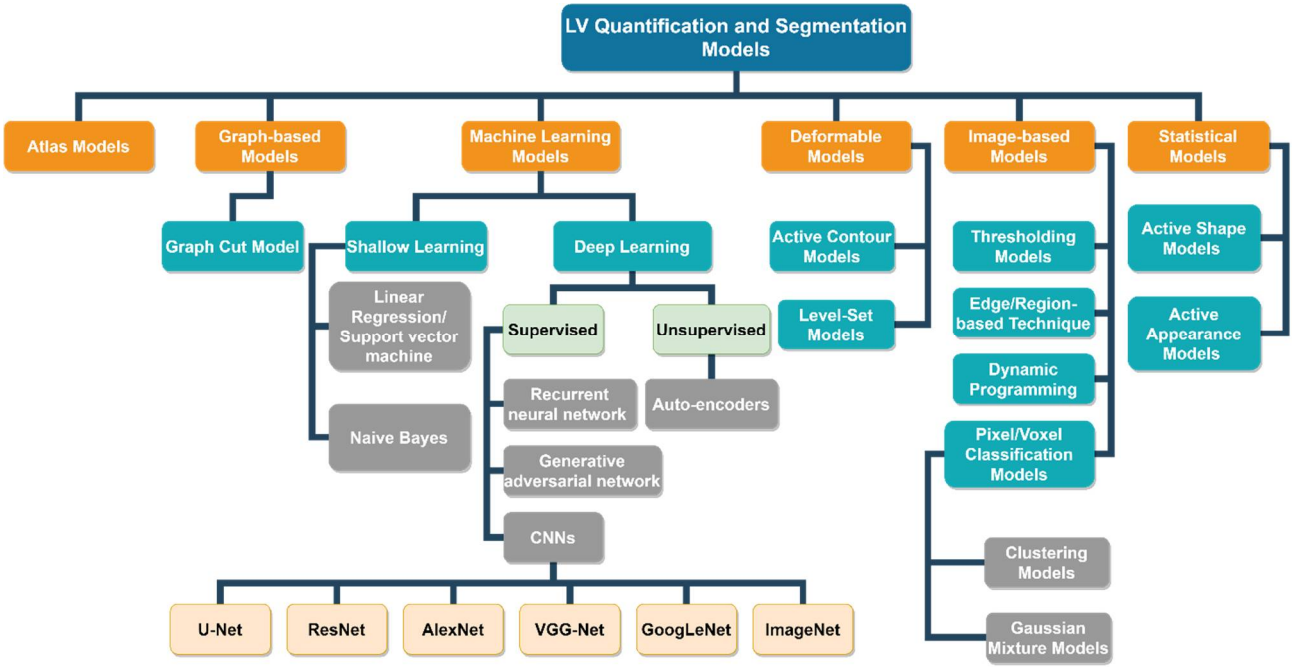

Figure 5. Taxonomy of LV segmentation models

LV Quantification

Existing methods for LV motion estimation in cine MR imaging are divided into three categories: image-based, feature tracking and deformable models. Recently, deep learning algorithms played an important role in LV quantification [66, 67] to predict critical diseases such as myocardial infarction from MRI [68, 69]. In the LV quantification, the multi-task learning framework model is widely utilised [21]. The model, which performs both LV parameter estimation and myocardium segmentation, was first proposed by Chen et al. [10], and it is known as the deep multi-task conditional quantification network. The framework consists of a U-net segmentation model and a quantification encoder with consecutive convolutional layers. This method has a limitation in terms of the number of segmentation labels required for training; thus, using unsupervised algorithms to improve framework adaptation was suggested.

Khened et al. [53] presented a multi-scale residual DenseNet to combine both segmentation and diagnosis of cardiac disease; this network is based on an FCN. They proposed the inception module's parallel structures for image processing input at multiple scales and viewpoints simultaneously. This work demonstrated a computational vision technique for the detection of segmentation of the region of interest in the end-to-end deep learning. Clinical cardiac parameters were extracted from the segmentation maps to demonstrate the analysis of clinical diagnosis and the ensemble classifiers that were trained to classify cardiac disease. Dong et al. [70] proposed two parallel end-to-end CNNs to detect both LV contours using the concept of multi-task learning.

The full quantification of the LV is based on the simultaneous measurement of the LV volume and mass, six regional wall thicknesses, three LV dimensions and the diastole or systole

phase. However, as mentioned by Xue et al. [21], the full LV quantification is a difficult task due to: (1) the high variability of cardiac structure that leads to inhomogeneity of cardiac appearance; (2) the complexity during the cardiac cycle of determining myocardium's temporal deformation; and (3) the mysterious relationship between different indices. The same group of researchers proposed a deep multi-task relationship learning network to quantify the LV from short-axis MRI. The proposed method included four integrated modules: the CNN to represent cardiac images, two parallel recurrent neural networks for modelling the temporal dynamics of cardiac sequences, and the soft-max classifier for estimation of the LV indices. Yang et al. [71] proposed a high-accuracy and stable technique to locate the LV at ED and ES phases using CNN in the free-breathing MRI. Tao et al. [72] created a CNN model for the LV quantification using short-axis cine MRI in multicentre and multivendor settings.

LV Segmentation

Cardiac MRI present the patient's heart with surrounding chest cavity organs such as the lungs and diaphragm [53]. The region-of-interest detection step is proposed to approximately localise the heart region, e.g. the LV cavity in MRI. The region-of-interest extraction of LV features is extensively used in the training and inference of deep learning models [73-75]. In computer-aided diagnosis, the localisation of the LV in MRI plays a crucial role in diagnosing heart disease. Based on CNN regression and deep distance metric learning, Wang et al. [67] proposed a method for LV localisation and identification from cardiac MRI. They employed a combined distance metric learning and super-pixel segmentation algorithm to ignore handcrafted features and learn deep-patch feature representation. Besides, a salient patch module with two channels was proposed to prevent low discrimination of image regions. The CNN regression module was created for landmark localisation by combining the weights of three networks, and the LV was further recognised by Mean Shift algorithm. Although this method achieved higher accuracy in LV localisation from the cardiac MRI, a single CNN regression did not adapt to the huge differences in MRI effectively. Methods of cascading CNN regression and classification should be investigated to address this issue. Tan et al. [20] presented an automated module for LV segmentation based on CNN regression and used two approaches: LV centre-point localisation and determination of the LV border radii in polar space.

LV segmentation is a critical task for determining clinical parameters such as LV mass and volume as well as the diagnosis of cardiovascular pathologies [76]. Nonetheless, this task remains difficult for the following reasons, as listed by Wang et al. [19]: (1) difficulty in distinguishing between myocardium and papillary muscles with similar intensities; (2) variations in brightness in the LV cavity due to blood flow; (3) complex segmentation of apical and basal slices; (4) personal variability in LV shapes and intensities; and (5) noise associated with cine MRI. Zhang et al. [77] first proposed a method for the automatic detection of missing apical and basal slices of MRI, which affects the diagnostic accuracy of LV quantification, by introducing a novel Fisher-discriminative 3D CNN classifiers.

Many LV conventional segmentation approaches have been conducted, as mentioned previously. However, all of the models depend on the initial model placement with undesired local minima of the objective function [8]. CNNs have been used extensively for a successful classification and segmentation with high performance. Moreover, hybrid approaches that include deep learning-based and model-based ones are utilised for accurate LV quantification/segmentation. Hu et al. [44] proposed a hybrid method of constructing a 3D-active shape model automatically for

Maejo Int. J. Sci. Technol. **2021**, *15*(03), 273-292

the LV, in which the CNNs were used to obtain the initial shape of the LV, and point distribution models were utilised to derive the distance maps from the ground truth of endocardial and epicardial contours. This study found that combining deep learning and statistical models is beneficial for LV functional parameters evaluation.

Further, Avendi et al. [78] proposed a hybrid approach of deep learning and deformable models to reducing the complex problem of LV segmentation. The method was achieved in three stages: determining the region of interest of the LV using CNN; stacking auto-encoders to detect the LV's shape; and using deformable models to optimise the accuracy of the segmentation. The testing of this method on a larger clinical data set was suggested for researchers in the future to enhance the network performance. Resolving critical segmentation issues, hybrid models have demonstrated significant potential in LV segmentation. Indeed, Lan et al. [6] employed this technique by combining CNN and snake models in automatic LV segmentation using MRI. The CNN was used to segment the LV and two double snake models were utilised to assess endocardial and epicardial boundaries. Wu et al. [79] developed a hybrid technique by combining CNN and U-net models to locate the region of interest and segment the LV. Despite the high accuracy of their model, only non-professional diastolic and systolic segmentation of LV boundaries exists. Lin et al. [55] proposed the first data augmentation approach to improve the model performance by training the FCN from few samples for LV segmentation using shape models. One issue with LV segmentation is a small annotated training data set where the visual region of interest requires variations in large shape and appearance. Ngo et al. [80] solved this problem by combining deep learning with a level set for automated LV segmentation from cine MRI.

Based on the hybrid techniques with deep learning algorithms, Wu et al. [23] were the first to employ graph matching based on a feature point descriptor using FCN to estimate cardiac motion. Using an FCN, they first segmented the LV's endocardial contour and extracted point features. Then, in graph matching, they employed a feature descriptor with the FCN to estimate the LV motion. During the construction of graphs representing the LV's endocardial contour, the graph matching algorithm hypothesised that the LV contour is the same as a circle. When the LV contours are abnormal, the performance of graph matching model is poor. An overview of segmentation techniques using short-axis cardiac MRI based on non-learning-based algorithms from 1993 to 2010 can be observed in the work of Petitjean and Dacher [81] with more enriched information on the LV and RV, while the study by Fahmy et al. [82] summarised the segmentation of the heart's chambers from MRI, ultrasonic, and computed tomography data sets. These works prove that the segmentation of the LV using short-axis MRI is the most crucial method in heart disease diagnosis nowadays.

Cardiac MRI Data Sets

Several sources of cardiac MRI data sets are used for LV segmentation and quantification, including the automatic cardiac diagnosis challenge (ACDC), the left ventricle segmentation challenge (LVSC), the Sunnybrook cardiac data (SCD) and York and cardiac Kaggle data sets. Table 1 outlines the details of these data sets; additionally, Bernard et al. [9] summarised a comparison of existing cardiac MRI data sets.

Maejo Int. J. Sci. Technol. **2021**, *15*(03), 273-292

Table 1. Cine MRI public data sets for LV and myocardial segmentation

MRI data sets			
Datasets name	**Year**	**No. of subjects**	**Main pathology**
ACDC [9]	2017	150	myocardial infarction and hypertrophic cardiomyopathy
SCD [83]	2009	45	hypertrophy, heart failure with/without infarction and cardiomyopathy
LVSC [84]	2011	200	coronary artery disease and myocardial infarction
York [85]	2008	33	cardiomyopathy, enlarge ventricles, aortic regurgitation and ischemia
Kaggle [86]	2015	700	Measuring ED and ES volumes

COMPARISON AND DISCUSSION

Table 2 tabulates an overview of the current methods based on the tasks of the LV segmentation and quantification from various MRI data sets. Comparative analysis was used in terms of methods and types of cardiac MRI. It can be observed that the CNN U-Net-based architecture is the most used among these methods that combine with models such as active contours and deformable models. Moreover, deformable models that infer the LV shape combined with a deep learning algorithm were proposed by Avendi et al. [78] for automatic LV segmentation. Similarly, Ngo et al. [80] and Xie et al. [18] improved the accuracy of the segmentation network by combining the level set approaches with a deep learning algorithm.

Further, Wu [23] utilised deep learning algorithms together with graph matching to estimate the LV motion, whereas Wang [19] used a dynamic pixel-wise weighting approach in conjunction with a CNN model for LV segmentation. Hu [44] also employed hybrid models to construct a 3D shape for the LV by combining a 3D active shape model with a CNN algorithm. Recently, Lan and Jin [6] combined a snake model (active contour) with the CNN algorithm, achieving better segmentation accuracy than all previous models. Table 3 shows a quantitative analysis of the most recent methods through different evaluation metrics, namely dice metrics, average perpendicular dice (APD), and good of contours percentage. The performance of the model proposed by Lan and Jin [6] outperforms other existing methods with dice metrics of 0.96 and 0.97 for endocardial and epicardial contours respectively, followed by the model of Wu et al. [79] with a dice metric of 0.95 for both contours. Combining the deep learning-based algorithms with traditional feature-guided models thus results in robust models for LV segmentation and quantification from MRI.

Maejo Int. J. Sci. Technol. **2021**, *15*(03), 273-292

Table 2. Overview of current studies on LV segmentation from MRI data sets

Author /year	Objective	Method	Database
Wu et al. 2020 [23]	LV motion estimation	Graph matching + FCNs	LVSC (MICCAI 2009)
Romaguera et al. 2018 [87]	Myocardium segmentation	FCN + six optimisation algorithm comparison	SCD
Zheng et al. 2019 [88]	LV motion characterisation	Apparent flow of semi-supervised learning	ACDC
Ngo et al. 2017 [80]	LV segmentation	Deep learning + level set methods	LVSC (MICCAI 2009)
Wang et al. 2020 [19]	LV segmentation	Dynamic pixel-wise weighting + CNN	LVSC (MICCAI 2013)
Chen et al. 2020 [10]	LV quantification	Deep multi-task + U-net	LVSC (MICCAI 2018)
Wu et al. 2020 [79]	LV segmentation	CNN U-net based architecture	LVSC (MICCAI 2009)
Curiale et al. 2019 [8]	LV quantification	CNN U-net based architecture	SCD and CAP
Khened et al. 2019 [53]	Myocardium segmentation	DenseNet based FCN architecture	ACDC-2017, LVSC-2011 and Kaggle
Tan et al. 2017 [20]	LV segmentation	CNN regression model	LVSC (MICCAI 2011)
Wang et al. 2020 [67]	LV landmark localisation	CNN regression + classification models	CAP
Hu et al. 2020 [44]	LV 3D-ASM	CNN + 3D-ASM	1200 MRI from Hubei cancer hospital
Lan and Jin 2019 [6]	LV segmentation	CNN + active contour (snake model)	Sunnybrook
Tao et al. 2019 [72]	LV quantification	CNN U-net based architecture	596 MRI collected from medical centres
Lin et al. 2020 [55]	LV segmentation	FCN + shape model	MICCAI 2009, CAP, Kaggle and 33 subjects
Dong et al. 2020 [70]	LV segmentation	Two parallel end-to-end CNNs	LVSC (MICCAI 2019)
Yang et al. 2017 [89]	LV segmentation	CS-FCM	Sunnybrook
Xie et al. 2020 [18]	LV segmentation	CNN + level set model	MICCAI 2009 and MICCAI 2017
Avendi et al. 2016 [78]	LV segmentation	CNN + deformable model	LVSC (MICCAI 2009)

Note: ASM = active shape model, CAP = cardiac atlas project, FCM = fuzzy c-mean, MICCAI = international conference on medical image computing and computer-assisted intervention)

Maejo Int. J. Sci. Technol. **2021**, *15*(03), 273-292

Table 3. Comparative analysis of current studies on LV segmentation

Author	Dice metric		APD (mm)		Good (%)	
	Endo	Epi	Endo	Epi	Endo	Epi
Ngo et al. 2017 [80]	0.91 (0.03)	0.94 (0.02)	1.73 (0.31)	1.76 (0.40)	100 (0.0)	100 (0.0)
Romaguera et al. 2018 [87]	0.92 (0.01)	0.93 (0.02)	2.23 (0.31)	2.13 (0.28)	94.19 (7.38)	95.64 (7.11)
Avendi et al. 2016 [78]	0.94 (0.02)	-	1.81 (044)	-	96.69 (5.7)	-
Du et al. 2018 [90]	0.92 (0.04)	0.94 (0.02)	-	-	-	-
Lan and Jin 2019 [6]	0.96 (0.03)	0.97 (0.02)	1.81 (0.35)	1.84 (0.63)	97.08 (7.0)	97.91 (6.5)
Wu et al. 2020 [79]	0.95 (0.01)	0.95 (0.01)	-	-	-	-
Yang et al. 2017 [16]	0.92 (0.02)	0.94 (0.02)	1.77 (0.32)	1.85 (0.38)	-	-
Santiago et al. 2018 [47]	0.86 (0.08)	-	2.1 (0.7)	-	88.8	-
Dharanibai et al. 2018 [48]	0.88 (0.05)	0.93 (0.02)	1.94 (0.45)	1.96 (0.41)	99.57	98.98
Tao et al. 2019 [72]	0.95 (0.02)	0.96 (0.02)	1.3 (0.63)	1.3 (0.63)	-	-
Wang et al. 2020 [19]	0.80 (0.2)	0.80 (0.2)	-	-	-	-
Lin et al. 2020 [55]	0.88	0.94	2.38	2.08	89.81	94.19
Hu et al. 2019 [27]	0.90 (0.03)	0.93 (0.02)	1.95 (0.48)	1.98 (0.53)	96.80 (7.0)	98.4 (6.5)
Yang et al. 2017 [89]	0.89 (0.03)	-	2.23 (0.5)	-	-	-
Yang et al. 2020 [91]	0.94 (0.05)	0.94 (0.05)	-	-	-	-
Abdeltawab et al. 2020 [92]	0.92	0.96	-	-	-	-
Dong et al. 2020 [70]	0.95	0.96	-	-	-	-
Xie et al. 2020 [18]	0.90 (0.03)	0.95 (0.01)	2.02 (0.56)	1.63 (0.31)	94.59 (8.41)	96.88 (5.44)

Note: Endo=endocardium, Epi=epicardium. Figures indicate mean and (standard deviation).

CONCLUSIONS

Short-axis MRI have demonstrated high potential for segmenting LV parameters, particularly the myocardial wall thickness. Various existing CNN algorithms have also demonstrated satisfactory functionality in LV automatic segmentation of the short-axis MRI that diagnose cardiac disease at an early stage. By combining CNN models with statistical models or shape models such as active contours or deformable models, a robust hybrid model for LV segmentation and quantification can be produced. This paper presents different evaluation parameters that are beneficial not only for readers to develop a new scope of research, but also for clinicians to diagnose the cardiac disease accurately.

ACKNOWLEDGEMENTS

Communication of this research is made possible through monetary assistance by Universiti Tun Hussein Onn Malaysia, the UTHM Publisher's Office via Publication Fund E15216 and Fundamental Research Grant Scheme (FRGS/1/2020/TK0/UTHM/02/16).

REFERENCES

1. World Health Organization (WHO), "Cardiovascular diseases (CVDs)", **2016**, https://www.who.int/news-room/fact-sheets/detail/cardiovascular-diseases-(cvds) (Accessed: May 2021).
2. P. Piras, L. Teresi, P. E. Puddu, C. Torromeo, A. A. Young, A. Suinesiaputra and P. Medrano-Gracia, "Morphologically normalized left ventricular motion indicators from MRI feature tracking characterize myocardial infarction", *Sci. Rep.*, **2017**, *7*, Art.no.12259.

3. J. K. Kim and S. Kang, "Neural network-based coronary heart disease risk prediction using feature correlation analysis", *J. Healthcare Eng.*, **2017**, *2017*, Art.no.2780501.
4. R. Tao, S. Zhang, X. Huang, M. Tao, J. Ma, S. Ma, C. Zhang, T. Zhang, F. Tang, J. Lu, C. Shen and X. Xie, "Magnetocardiography-based ischemic heart disease detection and localization using machine learning methods", *IEEE Trans. Biomed. Eng.*, **2019**, *66*, 1658-1667.
5. G. Swapna, K. P. Soman and R. Vinayakumar, "Automated detection of cardiac arrhythmia using deep learning techniques", *Procedia Comput. Sci.*, **2018**, *132*, 1192-1201.
6. Y. Lan and R. Jin, "Automatic segmentation of the left ventricle from cardiac MRI using deep learning and double snake model", *IEEE Access*, **2019**, *7*, 128641-128650.
7. M. Porumb, E. Iadanza, S. Massaro and L. Pecchia, "A convolutional neural network approach to detect congestive heart failure", *Biomed. Sign. Process. Control*, **2020**, *55*, Art.no.101597.
8. A. H. Curiale, F. D. Colavecchia and G. Mato, "Automatic quantification of the LV function and mass: A deep learning approach for cardiovascular MRI", *Comput. Meth. Programs Biomed.*, **2019**, *169*, 37-50.
9. O. Bernard, A. Lalande, C. Zotti, F. Cervenansky, X. Yang, P.-A. Heng, I. Cetin, K. Lekadir, O. Camara, M. A. G. Ballester, G. Sanroma, S. Napel, S. Petersen, G. Tziritas, E. Grinias, M. Khened, V. A. Kollerathu, G. Krishnamurthi, M.-M. Rohe, X. Pennec, M. Sermesant, F. Isensee, P. Jager, K. H. Maier-Hein, P. M. Full, I. Wolf, S. Engelhardt, C. F. Baumgartner, L. M. Koch, J. M. Wolterink, I. Isgum, Y. Jang, Y. Hong, J. Patravali, S. Jain, O. Humbert and P.-M. Jodoin, "Deep learning techniques for automatic MRI cardiac multi-structures segmentation and diagnosis: Is the problem solved?", *IEEE Trans. Med. Imaging*, **2018**, *37*, 2514-2525.
10. R. Chen, C. Xu, Z. Dong, Y. Liu and X. Du, "DeepCQ: Deep multi-task conditional quantification network for estimation of left ventricle parameters", *Comput. Meth. Programs Biomed.*, **2020**, *184*, Art.no.105288.
11. P. Peng, K. Lekadir, A. Gooya, L. Shao, S. E. Petersen and A. F. Frangi, "A review of heart chamber segmentation for structural and functional analysis using cardiac magnetic resonance imaging", *Magn. Reson. Mater. Phys. Biol. Med.*, **2016**, *29*, 155-195.
12. C. Chen, C. Qin, H. Qiu, G. Tarroni, J. Duan, W. Bai and D. Rueckert, "Deep learning for cardiac image segmentation: A review", *Front. Cardiovasc. Med.*, **2020**, *7*, Art.no.25.
13. A. Krasnobaev and A. Sozykin, "An overview of techniques for cardiac left ventricle segmentation on short-axis MRI", *ITM Web Conf.*, **2016**, *8*, Art.no.01003.
14. A. R. Patel and C. M. Kramer, "Role of cardiac magnetic resonance in the diagnosis and prognosis of nonischemic cardiomyopathy", *JACC Cardiovasc. Imaging*, **2017**, *10*, 1180-1193.
15. L. K. Tan, Y. M. Liew, E. Lim, Y. F. A. Aziz, K. H. Chee and R. A. McLaughlin, "Automatic localization of the left ventricular blood pool centroid in short axis cardiac cine MR images", *Med. Biol. Eng. Comput.*, **2018**, *56*, 1053-1062.
16. C. Yang, W. Wu, Y. Su and S. Zhang, "Left ventricle segmentation via two-layer level sets with circular shape constraint", *Magn. Reson. Imaging*, **2017**, *38*, 202-213.
17. A. Budai, F. I. Suhai, K. Csorba, A. Toth, L. Szabo, H. Vago and B. Merkely, "Fully automatic segmentation of right and left ventricle on short-axis cardiac MRI images", *Comput. Med. Imaging Graph.*, **2020**, *85*, Art.no.101786.
18. L. Xie, Y. Song and Q. Chen, "Automatic left ventricle segmentation in short-axis MRI using deep convolutional neural networks and central-line guided level set approach", *Comput. Biol. Med.*, **2020**, *122*, Art.no.103877.

19. Z. Wang, L. Xie and J. Qi, "Dynamic pixel-wise weighting-based fully convolutional neural networks for left ventricle segmentation in short-axis MRI", *Magn. Reson. Imaging*, **2020**, *66*, 131-140.
20. L. K. Tan, Y. M. Liew, E. Lim and R. A. McLaughlin, "Convolutional neural network regression for short-axis left ventricle segmentation in cardiac cine MR sequences", *Med. Image Anal.*, **2017**, *39*, 78-86.
21. W. Xue, G. Brahm, S. Pandey, S. Leung and S. Li, "Full left ventricle quantification via deep multitask relationships learning", *Med. Image Anal.*, **2018**, *43*, 54-65.
22. Nayak, S. Krishna, J. F. Nielsen, A. B. Matt, M. Markl, D. G. Peter, M. B. Rene, S. David , C. Lorenz, H. Wen, S. H. Bob, H. E. Frederick, N. O. John, and V. R. Subha, "Cardiovascular magnetic resonance phase contrast imaging", *J. Cardiovasc. Magn. Reson.,* **2015**, *17*, Art.no.71.
23. J. Wu, Z. Gan, W. Guo, X. Yang and A. Lin, "A fully convolutional network feature descriptor: Application to left ventricle motion estimation based on graph matching in short-axis MRI", *Neurocomput.*, **2020**, *392*, 196-208.
24. A. Krizhevsky, I. Sutskever and G. E. Hinton, "ImageNet classification with deep convolutional neural networks", *Commun. ACM*, **2017**, *60*, 84-90.
25. K. Alsaih, M. Z. Yusoff, T. B. Tang, I. Faye and F. Mériaudeau, "Deep learning architectures analysis for age-related macular degeneration segmentation on optical coherence tomography scans", *Comput. Meth. Programs Biomed.*, **2020**, *195*, Art.no.105566.
26. S. Ren, K. He, R. Girshick and J. Sun, "Faster R-CNN: Towards real-time object detection with region proposal networks", *IEEE Trans. Pattern Anal. Mach. Intell.*, **2017**, *39*, 1137-1149.
27. H. Hu, N. Pan, J. Wang, T. Yin and R. Ye, "Automatic segmentation of left ventricle from cardiac MRI via deep learning and region constrained dynamic programming", *Neurocomput.*, **2019**, *347*, 139-148.
28. F. F. Ting, Y. J. Tan and K. S. Sim, "Convolutional neural network improvement for breast cancer classification", *Expert Syst. Appl.*, **2019**, *120*, 103-115.
29. S. Dabeer, M. M. Khan and S. Islam, "Cancer diagnosis in histopathological image: CNN based approach", *Inform. Med. Unlocked*, **2019**, *16*, Art.no.100231.
30. A. K. Anaraki, M. Ayati and F. Kazemi, "Magnetic resonance imaging-based brain tumor grades classification and grading via convolutional neural networks and genetic algorithms", *Biocybern. Biomed. Eng.*, **2019**, *39*, 63-74.
31. A. Nithya, A. Appathurai, N. Venkatadri, D. R. Ramji and C. A. Palagan, "Kidney disease detection and segmentation using artificial neural network and multi-kernel k-means clustering for ultrasound images", *Measure.*, **2020**, *149*, Art.no.106952.
32. S. Wan, Y. Liang and Y. Zhang, "Deep convolutional neural networks for diabetic retinopathy detection by image classification", *Comput. Electr. Eng.*, **2018**, *72*, 274-282.
33. Z. Khan, N. Yahya, K. Alsaih, S. S. A. Ali and F. Meriaudeau, "Evaluation of deep neural networks for semantic segmentation of prostate in T2W MRI", *Sensors*, **2020**, *20*, Art.no.3183.
34. M. Baldeon-Calisto and S. K. Lai-Yuen, "AdaResU-Net: Multiobjective adaptive convolutional neural network for medical image segmentation", *Neurocomput.*, **2020**, *392*, 325-340.
35. S. L. Oh, E. Y. K. Ng, R. S. Tan and U. R. Acharya, "Automated diagnosis of arrhythmia using combination of CNN and LSTM techniques with variable length heart beats", *Comput. Biol. Med.*, **2018**, *102*, 278-287.
36. J. Aoe, R. Fukuma, T. Yanagisawa, T. Harada, M. Tanaka, M. Kobayashi, Y. Inoue, S.

Yamamoto, Y. Ohnishi and H. Kishima, "Automatic diagnosis of neurological diseases using MEG signals with a deep neural network", *Sci. Rep.*, **2019**, *9*, Art.no.5057.

37. J. J. Nirschl, A. Janowczyk, E. G. Peyster, R. Frank, K. B. Margulies, M. D. Feldman and A. Madabhushi, "A deep-learning classifier identifies patients with clinical heart failure using whole-slide images of H and E tissue", *PLoS One*, **2018**, *13*, Art.no.e0192726.
38. T. Li, B. Wei, J. Cong, Y. Hong and S. Li, "Direct estimation of left ventricular ejection fraction via a cardiac cycle feature learning architecture", *Comput. Biol. Med.*, **2020**, *118*, Art.no.103659.
39. V. Badrinarayanan, A. Kendall and R. Cipolla, "SegNet: A deep convolutional encoder-decoder architecture for image segmentation", *IEEE Trans. Pattern Anal. Mach. Intell.*, **2017**, *39*, 2481-2495.
40. Y. Lecun, Y. Bengio and G. Hinton, "Deep learning", *Nature*, **2015**, *521*, 436-444.
41. D. P. Kingma and J. L. Ba, "ADAM: A method for stochastic optimization", Proceedings of 3rd International Conference on Learning Representations, **2015**, San Diego, USA (arXiv preprint arXiv:1412.6980).
42. F. Milletari, N. Navab and S.-A. Ahmadi, "V-Net: Fully convolutional neural networks for volumetric medical image segmentation", Proceedings of 4th International Conference on 3D Vision (3DV), **2016**, Standford, USA, pp.565-571.
43. K. He, X. Zhang, S. Ren and J. Sun, "Deep residual learning for image recognition", Proceedings of IEEE Conference on Computer Vision and Pattern Recognition, **2016**, Las Vegas, USA, pp.770-778.
44. H. Hu, N. Pan, T. Yin, H. Liu and B. Du, "Hybrid method for automatic construction of 3D-ASM image intensity models for left ventricle", *Neurocomput.*, **2020**, *396*, 65-75.
45. S. V Stehman, "Selecting and interpreting measures of thematic classification accuracy", *Remote Sens. Environ.*, **1997**, *62*, 77-89.
46. J. Enguehard, P. O'Halloran and A. Gholipour, "Semi-supervised learning with deep embedded clustering for image classification and segmentation", *IEEE Access*, **2019**, *7*, 11093-11104.
47. C. Santiago, J. C. Nascimento and J. S. Marques, "Fast segmentation of the left ventricle in cardiac MRI using dynamic programming", *Comput. Meth. Programs Biomed.*, **2018**, *154*, 9-23.
48. G. Dharanibai, A. Chandrasekharan and Z. C. Alex, "Automated segmentation of left ventricle using local and global intensity based active contour and dynamic programming", *Int. J. Autom. Comput.*, **2018**, *15*, 673-688.
49. C. Santiago, J. C. Nascimento and J. S. Marques, "A new ASM framework for left ventricle segmentation exploring slice variability in cardiac MRI volumes", *Neural Comput. Appl.*, **2017**, *28*, 2489-2500.
50. L. Li, F. Wu, G. Yang, L. Xu, T. Wong, R. Mohiaddin, D. Firmin, J. Keegan and X. Zhuang, "Atrial scar quantification via multi-scale CNN in the graph-cuts framework", *Med. Image Anal.*, **2020**, *60*, Art.no.101595.
51. G. Farrar, A. Suinesiaputra, K. Gilbert, J. C. Perry, S. Hegde, A. Marsden, A. A. Young, J. H. Omens and A. D. McCulloch, "Atlas-based ventricular shape analysis for understanding congenital heart disease", *Progr. Pediatr. Cardiol.*, **2016**, *43*, 61-69.
52. X. Zhuang and J. Shen, "Multi-scale patch and multi-modality atlases for whole heart segmentation of MRI", *Med. Image Anal.*, **2016**, *31*, 77-87.
53. M. Khened, V. A. Kollerathu and G. Krishnamurthi, "Fully convolutional multi-scale residual

DenseNets for cardiac segmentation and automated cardiac diagnosis using ensemble of classifiers", *Med. Image Anal.*, **2019**, *51*, 21-45.

54. H. C. Shin, H. R. Roth, M. Gao, L. Lu, Z. Xu, I. Nogues, J. Yao, D. Mollura and R. M. Summers, "Deep convolutional neural networks for computer-aided detection: CNN architectures, dataset characteristics and transfer learning", *IEEE Trans. Med. Imaging*, **2016**, *35*, 1285-1298.
55. A. Lin, J. Wu and X. Yang, "A data augmentation approach to train fully convolutional networks for left ventricle segmentation", *Magn. Reson. Imaging*, **2020**, *66*, 152-164.
56. M. Nasr-Esfahani, M. Mohrekesh, M. Akbari, S. M. R. Soroushmehr, E. Nasr-Esfahani, N. Karimi, S. Samavi, and K. Najarian, "Left ventricle segmentation in cardiac MR images using fully convolutional network", Proceedings of 40th Annual International Conference of the IEEE Engineering in Medicine and Biology Society, **2018**, Honolulu, USA, pp.1275-1278.
57. W. Bai, M. Sinclair, G. Tarroni, O. Oktay, M. Rajchl, G. Vaillant, A. M. Lee, N. Aung, E. Lukaschuk, M. M. Sanghvi, F. Zemrak, K. Fung, J. M. Paiva, V. Carapella, Y. J. Kim, H. Suzuki, B. Kainz, P. M. Matthews, S. E. Petersen, S. K. Piechnik, S. Neubauer, B. Glocker and D. Rueckert, "Automated cardiovascular magnetic resonance image analysis with fully convolutional networks", *J. Cardiovasc. Magn. Reson.*, **2018**, *20*, Art.no.65.
58. V. Turchenko and A. Luczak, "Creation of a deep convolutional auto-encoder in Caffe", Proceedings of 9th IEEE International Conference on Intelligent Data Acquisition and Advanced Computing Systems: Technology and Applications, **2017**, Bucharest, Romania, pp.651-659.
59. A. Creswell, T. White, V. Dumoulin, K. Arulkumaran, B. Sengupta and A. A. Bharath, "Generative adversarial networks: An overview", *IEEE Sign. Process. Magaz.*, **2018**, *35*, 53-65.
60. J. Long, E. Shelhamer and T. Darrell, "Fully convolutional networks for semantic segmentation", Proceedings of IEEE Conference on Computer Vision and Pattern Recognition, **2015**, Boston, USA, pp.3431-3440.
61. O. Ronneberger, P. Fischer and T. Brox, "U-net: Convolutional networks for biomedical image segmentation", *Lect. Notes Comput. Sci.*, **2015**, *9351*, 234-241.
62. K. Cho, B. van Merrienboer, C. Gulcehre, D. Bahdanau, F. Bougares, H. Schwenk and Y. Bengio, "Learning phrase representations using RNN encoder-decoder for statistical machine translation", Proceedings of Conference on Empirical Methods in Natural Language Processing, **2014**, Doha, Qatar, pp.1724-1734.
63. I. J. Goodfellow, J. Pouget-Abadie, M. Mirza, B. Xu, D. Warde-Farley, S. Ozair, A. Courville and Y. Bengio, "GAN（Generative Adversarial Nets）", *J. Japan Soc. Fuzzy Theory Intell. Inform.*, **2017**, *29*, 177-177.
64. V. K. Singh, H. A. Rashwan, S. Romani, F. Akram, N. Pandey, Md. M. K. Sarker, A. Saleh, M. Arenas, M. Arquez, D. Puig and J. Torrents-Barrena, "Breast tumor segmentation and shape classification in mammograms using generative adversarial and convolutional neural network", *Expert Syst. Appl.*, **2020**, *139*, Art.no.112855.
65. X. Zhen, Z. Wang, A. Islam, M. Bhaduri, I. Chan and S. Li, "Multi-scale deep networks and regression forests for direct bi-ventricular volume estimation", *Med. Image Anal.*, **2016**, *30*, 120-129.
66. B. Böttcher, E. Beller, A. Busse, D. Cantré, S. Yücel, A. Öner, H. Ince, M.-A. Weber and F. G.

Meinel, "Fully automated quantification of left ventricular volumes and function in cardiac MRI: Clinical evaluation of a deep learning-based algorithm", *Int. J. Cardiovasc. Imaging*, **2020**, *36*, 2239-2247.

67. X. Wang, S. Zhai and Y. Niu, "Left ventricle landmark localization and identification in cardiac MRI by deep metric learning-assisted CNN regression", *Neurocomput.*, **2020**, *399*, 153-170.
68. N. Zhang, G. Yang, Z. Gao, C. Xu, Y. Zhang, R. Shi, J. Keegan, L. Xu, H. Zhang, Z. Fan and D. Firmin, "Deep learning for diagnosis of chronic myocardial infarction on nonenhanced cardiac cine MRI", *Radiol.*, **2019**, *291*, 606-617.
69. M. Chen, L. Fang, Q. Zhuang and H. Liu, "Deep learning assessment of myocardial infarction from MR image sequences", *IEEE Access*, **2019**, *7*, 5438-5446.
70. Z. Dong, X. Du and Y. Liu, "Automatic segmentation of left ventricle using parallel end-end deep convolutional neural networks framework", *Knowledge-Based Syst.*, **2020**, *204*, Art.no.106210.
71. F. Yang, Y. He, M. Hussain, H. Xie and P. Lei, "Convolutional neural network for the detection of end-diastole and end-systole frames in free-breathing cardiac magnetic resonance imaging", *Comput. Math. Meth. Med.*, **2017**, *2017*, Art.ID1640835.
72. Q. Tao, W. Yan, Y. Wang, E. H. M. Paiman, D. P. Shamonin, P. Garg, S. Plein, L. Huang, L. Xia, M. Sramko, J. Tintera, A. de Roos, H. J. Lamb and R. J. van der Geest, "Deep learning-based method for fully automatic quantification of left ventricle function from cine MR images: A multivendor, multicenter study", *Radiol.*, **2019**, *290*, 81-88.
73. X. Du, S. Yin, R. Tang, Y. Zhang and S. Li, "Cardiac-DeepIED: Automatic pixel-level deep segmentation for cardiac bi-ventricle using improved end-to-end encoder-decoder network", *IEEE J. Transl. Eng. Health Med.*, **2019**, *7*, Art.no.1900110.
74. X. Du, R. Tang, S. Yin, Y. Zhang and S. Li, "Direct segmentation-based full quantification for left ventricle via deep multi-task regression learning network", *IEEE J. Biomed. Health Inform.*, **2019**, *23*, 942-948.
75. F. Liao, X. Chen, X. Hu and S. Song, "Estimation of the volume of the left ventricle from MRI images using deep neural networks", *IEEE Trans. Cybernet.*, **2019**, *49*, 495-504.
76. D. A. Iskandar, A. Khan, P. C. Lim and Y. C. Wang, "Automatic segmentation measuring function for cardiac MR-Left Ventricle (LV) images", *J. Telecommun. Electron. Comput. Eng.*, **2017**, *9*, 165-171.
77. L. Zhang, A. Gooya, M. Pereanez, B. Dong, S. K. Piechnik, S. Neubauer, S. E. Petersen and A. F. Frangi, "Automatic assessment of full left ventricular coverage in cardiac cine magnetic resonance imaging with Fisher-discriminative 3-D CNN", *IEEE Trans. Biomed. Eng.*, **2019**, *66*, 1975-1986.
78. M. R. Avendi, A. Kheradvar and H. Jafarkhani, "A combined deep-learning and deformable-model approach to fully automatic segmentation of the left ventricle in cardiac MRI", *Med. Image Anal.*, **2016**, *30*, 108-119.
79. B. Wu, Y. Fang and X. Lai, "Left ventricle automatic segmentation in cardiac MRI using a combined CNN and U-net approach", *Comput. Med. Imaging Graph.*, **2020**, *82*, Art.no.101719.
80. T. A. Ngo, Z. Lu and G. Carneiro, "Combining deep learning and level set for the automated segmentation of the left ventricle of the heart from cardiac cine magnetic resonance", *Med. Image Anal.*, **2017**, *35*, 159-171.

81. C. Petitjean and J. N. Dacher, "A review of segmentation methods in short axis cardiac MR images", *Med. Image Anal.*, **2011**, *15*, 169-184.
82. A. S. Fahmy, H. El-Rewaidy, M. Nezafat, S. Nakamori and R. Nezafat, "Automated analysis of cardiovascular magnetic resonance myocardial native T1 mapping images using fully convolutional neural networks", *J. Cardiovasc. Magn. Reson.*, **2019**, *21*, Art.no.7.
83. P. Radau, Y. Lu, K. Connelly, G. Paul, A. J. Dick and G. A. Wright, "Evaluation framework for algorithms segmenting short axis cardiac MRI", *MIDAS J.*, **2009**, http://hdl.handle.net/10380/3070.
84. A. Suinesiaputra, B. R. Cowan, A. O. Al-Agamy, M. A. Elattar, N. Ayache, A. S. Fahmy, A. M. Khalifa, P. Medrano-Gracia, M.-P. Jolly, A. H. Kadish, D. C. Lee, J. Margeta, S. K. Warfield and A. A. Young, "A collaborative resource to build consensus for automated left ventricular segmentation of cardiac MR images", *Med. Image Anal.*, **2014**, *18*, 50-62.
85. A. Andreopoulos and J. K. Tsotsos, "Efficient and generalizable statistical models of shape and appearance for analysis of cardiac MRI", *Med. Image Anal.*, **2008**, *12*, 335-357.
86. Kaggle Dataset, "Second annual data science bowl challenge: Transforming how we diagnose heart disease", **2016**, https://www.kaggle.com/c/second-annual-data-science-bowl (Accessed: 24 October 2021).
87. L. V. Romaguera, F. P. Romero, C. F. F. C. Filho and M. G. F. Costa, "Myocardial segmentation in cardiac magnetic resonance images using fully convolutional neural networks", *Biomed. Signal Process. Control*, **2018**, *44*, 48-57.
88. Q. Zheng, H. Delingette and N. Ayache, "Explainable cardiac pathology classification on cine MRI with motion characterization by semi-supervised learning of apparent flow", *Med. Image Anal.*, **2019**, *56*, 80-95.
89. X. Yang, Q. Song and Y. Su, "Automatic segmentation of left ventricle cavity from short-axis cardiac magnetic resonance images", *Med. Biol. Eng. Comput.*, **2017**, *55*, 1563-1577.
90. X. Du, W. Zhang, H. Zhang, J. Chen, Y. Zhang, J. C. Warrington, G. Brahm and S. Li, "Deep regression segmentation for cardiac bi-ventricle MR images", *IEEE Access*, **2018**, *6*, 3828-3838.
91. Y. Yang, C. Feng and R. Wang, "Automatic segmentation model combining U-Net and level set method for medical images", *Expert Syst. Appl.*, **2020**, *153*, Art.no.113419.
92. H. Abdeltawab, F. Khalifa, F. Taher, N. S. Alghamdi, M. Ghazal, G. Beache, T. Mohamed, R. Keynton and A. El-Baz, "A deep learning-based approach for automatic segmentation and quantification of the left ventricle from cardiac cine MR images", *Comput. Med. Imaging Graph.*, **2020**, *81*, Art.no.101717.